Topics in Quantitative Finance Coursework

Subhag Pandit, Thomas Pink, Yaohuan Xie

June 9, 2025

In this project we will explore the methodology employed in the paper *Model-free Implied Volatility: From Surface to Index* by *M. Fukasawa, I. Ishida, N. Maghrebi et al* (hereafter referred to as "the paper") to estimate the expected quadratic variation of an asset at some future time T based on call and put option data.

1 Introduction

The quadratic variation of an asset can be used as a measure its volatility. Since there are many different methods of calculating the quadratic variation, we will specifically be looking at methods that are model-free. This means the methods will not assume that the implied volatility follows any specific model. Furthermore, the methods we will explore in this project use option prices to calculate the expected quadratic variation.

The Chicago Board of Exchange (CBOE) produces the VIX index, which used the following model-free formula to calculate the expected quadratic variation at time T of the S&P 500,

$$-2\mathbb{E}[\log(\frac{S_T}{F})] \approx 2\sum_{K=K_{min}}^{K_0-1}\frac{P(K)}{K^2}\Delta K + \frac{P(K_0)+C(K_0)}{K_0^2}\Delta K_0 + 2\sum_{K=K_0+1}^{K_{max}}\frac{C(K)}{K^2}\Delta K - (\frac{F}{K_0}-1)^2.$$

Here F represents the forward price and K_0 represents the strike closest to F. K_{min} is the minimum strike price available and K_{max} is the maximum. Also we have used $C(K)$ and $P(K)$ to represent the price of a call and put option with strike K respectively. This formula (which will now be called the CBOE procedure) comes from discretizing the following result,

$$-2\mathbb{E}[\log(\frac{S_T}{F})] = 2\int_0^{K_0}\frac{P(K)}{K^2}dK + 2\int_{K_0}^{F}\frac{K-F}{K^2}dK + 2\int_{K_0}^{\infty}\frac{C(K)}{K^2}dK. \tag{1}$$

The paper uses a different formulation to calculate the quadratic variation,

$$-\frac{2}{T}\mathbb{E}[\log(\frac{S_T}{F})] = \int_{-\infty}^{\infty}\sigma(g(z))^2\phi(z)dz. \tag{2}$$

Here, $\sigma(.)^2$ is the Black Scholes implied volatiltiy function and $g(.)$ is the inverse of the mapping $k \to d_2(k) = -\frac{k}{\sigma(k)\sqrt{T}} - \frac{\sigma(k)\sqrt{T}}{2}$. Also, $\phi(z)$ is the standard normal probability density function. The algorithm proposed in the paper begins by producing a polynomial to approximate the function $\sigma(g(z))^2$. Then it integrates this function against the standard normal p.d.f $\phi(z)$ directly, creating an estimate of higher accuracy than previous methods.

In this project, we will begin by deriving the key results in the paper including Equation 2 among other equations in Section 2. We will then explain the algorithm proposed by the paper in detail in Section 3, and define the other algorithms we will use in this paper for comparison in Section 4. In Sections 5 and 6 we will use simulated data and real data respectively, in order to test how well the method from the paper performs compared to other algorithms. We will then discuss some of the key aspects of the methodology in section 7 and critique the paper in Section 8. In Section 9, we explain the extensions we have explored as well as those that we did not have time to explore. Finally, in Section 10 we conclude our report.

2 Derivations

In this section we derive the key result from the paper using the same method used in the paper [FIM+11]. We begin by deriving the following result that will make calculating the expected quadratic variation much easier,

$$\log\left(\frac{S_T}{S_0}\right) = \int_0^T \frac{dS_t}{S_t} - \frac{1}{2}\int_0^T \frac{d\langle S\rangle_t}{S_t^2},$$
$$= \int_0^T \frac{dS_t^*}{S_t^*} + \log\left(\frac{S_T^0}{S_0^0}\right) - \frac{1}{2}\langle \log(S)\rangle_T.$$

Here S_t^0 is the value of the risk-less asset at time t, and $S_t^* = \frac{S_t}{S_t^0}$. The first line is due to ito's lemma and the second line is also due to Ito's lemma and the quadratic variation of an Ito's integral, by noticing that,

$$\langle f(X)\rangle_t = \int_0^t (f'(X_s))^2 d\langle X\rangle_s.$$

By taking expectations under the risk neutral measure, this derivation gives us the following key result,

$$\mathbb{E}[\langle \log S\rangle_T] = -2\mathbb{E}\left[\log\left(\frac{S_T}{S_0}\right)\right] + 2\mathbb{E}\left[\log\left(\frac{S_T^0}{S_0^0}\right)\right] = -2\mathbb{E}\left[\log\left(\frac{S_T}{\mathbb{E}(S_T)}\right)\right]$$

The RHS of this equation is what we will use in what follows to calculate the expected quadratic variation. We will now derive Equation 1. To begin with we define $F = \mathbb{E}(S_T)$, $C(K) = \mathbb{E}[(S_T - K)^+]$ and $P = \mathbb{E}[(K - S_T)^+]$. Then, using the fact that $C''(K) = P''(K)$ is the probability density function of the stock price by [BL78] we can derive Equation 1 using the following procedure,

$$-2\mathbb{E}\left[\log\left(\frac{S_T}{F}\right)\right] = -2\int_0^{K_0} \log\left(\frac{K}{F}\right) P''(K)dK - 2\int_{K_0}^{\infty} \log\left(\frac{K}{F}\right) C''(K)dK.$$

We now use integration by parts to get the following,

$$= -2\left[\log\left(\frac{K}{F}\right) P'(K)\right]_0^{K_0} + 2\int_0^{K_0} \frac{P'(K)}{K}dK - 2\left[\log\left(\frac{K}{F}\right) C'(K)\right]_{K_0}^{\infty} + 2\int_{K_0}^{\infty} \frac{C'(K)}{K}dK,$$

And then by using integration by parts again with the relation $\lim_{K\to\infty} C'(K) = \lim_{K\to 0} P'(K) = 0$ we get,

$$= -2\log\left(\frac{K_0}{F}\right)[P'(K_0) - C'(K_0)] + 2\left[\left[\frac{C(K)}{K}\right]_{K_0}^{\infty} + \int_{K_0}^{\infty} \frac{C(K)}{K^2}dK + \left[\frac{P(K)}{K}\right]_0^{K_0} + \int_0^{K_0} \frac{P(K)}{K^2}dK\right].$$

We now use the relation $P'(K) - C'(K) = 1$ (from differentiating put call parity) and $\lim_{K\to\infty} \frac{C(K)}{K} = \lim_{K\to 0} \frac{P(K)}{K} = 0$ (from L'hopital) to get the following result,

$$= 2\int_{K_0}^{\infty} \frac{C(K)}{K^2}dK + 2\int_0^{K_0} \frac{P(K)}{K^2}dK + 2\left[-\log\left(\frac{K_0}{F}\right) - \frac{C(K_0)}{K_0} + \frac{P(K_0)}{K_0}\right].$$

Finally, we use the put call parity, in this case $C(K) - P(K) = F - K$, to get,

$$= 2\int_{K_0}^{\infty} \frac{C(K)}{K^2}dK + 2\int_0^{K_0} \frac{P(K)}{K^2}dK + 2\left[-\log\left(\frac{K_0}{F}\right) + \frac{K_0 - F}{K_0}\right].$$

Thus we get Equation 1 by rewriting the value in the square brackets as an integral.

We will now begin deriving Equation 2. To begin with we state some definitions. Firstly, we set $K = Fe^k$ for some $k \in \mathbb{R}$. Next, we define $P_{BS}(k, \sigma)$ as the undiscounted Black-Scholes put option with strike K, maturity T and volatility $\sigma > 0$. We also define the function $D(K)$,

$$D(K) := \mathbb{E}[K > S_T] = \frac{dP}{dK}(K).$$

We now state some lemmas that we will prove in the Appendix.

Lemma 1 *For $\phi(.)$ the normal p.d.f,*

$$D(K) = D_{BS}(K) + \phi\left(-d_2\left(\log\left(\frac{K}{F}\right), \sigma\left(\log\left(\frac{K}{F}\right)\right)\right)\right)\frac{d\sigma}{dk}\left(\log\left(\frac{K}{F}\right)\right).$$

Lemma 2 *The mapping $k \to -d_2(k, \sigma(k))$ is increasing.*

Lemma 3 *If there exists $p > 0$ such that S_T^{-p} is integrable, then we have*

$$\lim_{k\to\pm\infty} \sigma(k)\phi(d_2(k,\sigma(k))) = 0 \quad \textit{and} \quad \lim_{k\to\pm\infty} k\frac{d\sigma}{dk}(k)\phi(d_2(k,\sigma(k))) = 0.$$

We now begin the derivation. Firstly, since the second derivative of $P(K)$ with respect to K is the same as the density of S_T, we notice,

$$-2\mathbb{E}\left[\log\left(\frac{S_T}{F}\right)\right] = -2\int_0^\infty \log\left(\frac{K}{F}\right)\frac{d^2P}{dK^2}(K)dK = -2\int_{-\infty}^\infty k\frac{d^2P}{dK^2}(Fe^k)Fe^k dk.$$

We now define the function g which is the inverse of d_2 from the Black-Scholes formula. This is well-defined since the mapping $k \to -d_2(k, \sigma(k))$ is increasing, from Lemma 2. We now use Lemma 1 to get,

$$\begin{aligned}
\frac{d^2P}{dK^2}(Fe^k) &= \frac{dD}{dK}(Fe^k), \\
&= \frac{d}{dK}\left(D_{BS}(K) + \phi\left(-d_2\left(\log\left(\frac{K}{F}\right), \sigma\left(\log\left(\frac{K}{F}\right)\right)\right)\right)\frac{d\sigma}{dk}\left(\log\left(\frac{K}{F}\right)\right)\right), \\
&= -\frac{1}{K}(\phi(g^{-1}(k)))\frac{dg^{-1}}{dk}(k) + \frac{1}{K}\frac{d}{dk}\left(\phi(-g^{-1}(k))\frac{d\sigma}{dk}(k)\right), \\
&= -\frac{1}{K}(\phi(g^{-1}(k)))\frac{dg^{-1}}{dk}(k) + \frac{1}{K}\left(-\frac{dg^{-1}}{dk}(k)\phi(-g^{-1}(k))\frac{d\sigma}{dk}(k) + \phi(-g^{-1}(k))\frac{d^2\sigma}{dk^2}(k)\right), \\
&= \frac{1}{Fe^k}\phi(g^{-1}(k))\left\{-\frac{dg^{-1}}{dk}(k)\left(1 + g^{-1}(k)\frac{d\sigma}{dk}(k)\right) + \frac{d\sigma^2}{dk^2}(k)\right\}.
\end{aligned}$$

Next, since

$$\frac{d}{dk}\phi(g^{-1}(k)) = -\phi(g^{-1}(k))g^{-1}(k)\frac{dg^{-1}}{dk}, \tag{3}$$

we get $\int -\phi(g^{-1}(k))g^{-1}(k)\frac{dg^{-1}}{dk}dk = \phi(g^{-1}(k))$. Thus using integration by parts we get,

$$\begin{aligned}
-\int_{-\infty}^\infty k\phi(g^{-1}(k))g^{-1}(k)\frac{dg^{-1}}{dk}(k)\frac{d\sigma}{dk}(k)dk = \\
\left[k\frac{d\sigma}{dk}(k)\phi(g^{-1}(k))\right]_{-\infty}^\infty - \int_{-\infty}^\infty \left\{\frac{d\sigma}{dk}(k) + k\frac{d^2\sigma}{dk^2}(k)\right\}\phi(g^{-1}(k))dk
\end{aligned}$$

Next, using Lemma 3, the square brackets cancels out. Thus we get,

$$-2\mathbb{E}\left[\log\left(\frac{S_T}{F}\right)\right] = 2\int_{-\infty}^\infty \left\{\frac{d\sigma}{dk}(k) + k\frac{dg^{-1}}{dk}(k)\right\}\phi(g^{-1}(k))dk. \tag{4}$$

We now notice,

$$\int_{-\infty}^\infty \phi(g^{-1}(k))\frac{d\sigma}{dk}(k)dk = [\phi(g^{-1}(k))\sigma(k)]_{-\infty}^\infty + \int_{-\infty}^\infty \phi(g^{-1}(k))g^{-1}(k)\sigma(k)\frac{dg^{-1}}{dk}(k)dk. \tag{5}$$

This result is due to integration by parts and Equation 3. Furthermore, we can also cancel out the square brackets by using Lemma 3 again. Then we substitute the following result,

$$\sigma(k)g^{-1}(k) = \sigma(k)\left[-\frac{k}{\sigma(k)} - \frac{\sigma(k)}{2}\right] = -k - \frac{\sigma(k)^2}{2}, \tag{6}$$

into Equation 5 and then into Equation 4. Here we have not included the $\sqrt{T}$ term, a further discussion is provided below. This results in two terms canceling in the integrand. Hence we are only left with the following,

$$\begin{aligned} -2\mathbb{E}\left[\log\left(\frac{S_T}{F}\right)\right] &= -\int_{-\infty}^{\infty} \phi(g^{-1}(k))\sigma(k)^2 \frac{dg^{-1}}{dk}(k)dk, \\ &= \int_{-\infty}^{\infty} \sigma(g(z))^2\phi(z)dz. \end{aligned}$$

In the last line we have used a change of basis using $z = g^{-1}(k)$ and the fact that $\lim_{t\to\pm\infty} g^{-1}(t) = \mp\infty$. This is not exactly the same as Equation 2, since it is missing a $\frac{1}{T}$ term. This is due to how we have defined d_2, without the $\sqrt{T}$ term. If we had added this in, Lemma 1 would change, with a $\sqrt{T}$ term in front of the p.d.f of the normal. Similarly, we would get another $\sqrt{T}$ from Equation 6. These together would cancel the $\frac{1}{T}$ term giving Equation 2 exactly.

3 The Algorithm

3.1 Algorithm Form

Note that throughout the report from now on, we refer to $\sigma(k)$ for the parameterisation of σ with respect to $k = \log\left(\frac{K}{F}\right)$, and via an abuse of notation $\sigma(d_2)$ for $\sigma(g(d_2))$.

The algorithm proposed in the paper [FIM+11] consists of the following steps.

1. Calculate the forward price
2. Select clean options data
3. Calculate implied volatilities $\sigma^2(k)$ and $d_2(k)$ for data
4. Ensure monotonicity of $d_2(k)$
5. Interpolate the volatility function $d_2 \to \sigma$
6. Take the expectation of $\sigma^2(d_2)$, with d_2 normally distributed

3.2 Calculate the Forward Price

In order to calculate the forward price, the paper [FIM+11] proposes finding the options that are closest to being at the money (where the put and call prices are closest to matching), using the most recent transaction price data. If no transactions are available for the option, they are not used.

Specifically the smallest of the strikes which have the smallest difference in most recent transaction price between the call and puts is taken as the at the money strike price. From the at the at the money strike price the forward price is calculated using the put call parity relation as follows:

$$K + e^{rT}\left(C_{\text{trans}}(K) - P_{\text{trans}}(K)\right)$$

3.3 Select Clean Options Data

In the paper, they ensure their options data is reasonable through the following two filters:

First they discard all options data where there is no bid data available, or no ask data available, as the midprice is necessary for the subsequent calculations.

Then where the the bid and ask prices are significantly different, the data is also discarded. Specifically, the paper discards all option data where the ask price is at least 2 times greater than the bid price.

3.4 Calculate Implied Volatilities

From the remaining options data, the implied volatility $\sigma(k)$ is calculated through use of a bisection algorithm method using the midprice of the retained option data. The corresponding value of $d_2(k)$ is then also calculated as,

$$d_2 = -\frac{k}{\sigma\sqrt{T}} - \frac{\sigma\sqrt{T}}{2}. \tag{7}$$

3.5 Ensure Monotonicity of d_2

$d_2(k)$ must be monotonically decreasing and so, starting from the at the money strike in both directions, any options data after and including the first strike that violates this condition is discarded.

3.6 Interpolate the volatility function

We interpolate the volatility function using a continuously differentiable interpolation. This is done using cubic splines between data points, and a constant approximation beyond the first and last piece of data. The paper makes use of a C^1 approximation, calculating it so that the gradient at adjacent points is such that the angle of incidence is equal to the angle of reflection in the horizontal plane parallel to the x axis where the gradients intersect. Specifically, they choose

$$y'(x_j) = -\left(\frac{\Delta x_j}{l_j} - \frac{\Delta x_{j-1}}{l_{j-1}}\right) \Bigg/ \left(\frac{\Delta y_j}{l_j} - \frac{\Delta y_{j-1}}{l_{j-1}}\right)$$

where

$$\Delta x_j = x_{j+1} - x_j$$
$$\Delta y_j = y_{j+1} - y_j$$
$$l_j = \sqrt{(\Delta x_j)^2 + (\Delta y_j)^2}$$

Denoting each polynomial as

$$y_i(x) = a_i + b_i(x - x_i) + c_i(x - x_i)^2 + d_i(x - x_i)^3$$

We then can compute the coefficients as follows

$$a_j = y(x_j)$$
$$b_j = y'(x_j)$$
$$c_j = \frac{3\Delta y_j - \Delta x_j b_{j+1} - 2\Delta x_j b_j}{\Delta x_j^2}$$
$$d_j = \frac{\Delta y_j - b_j \Delta x_j - c_j \Delta x_j^2}{\Delta x_j^3}$$

3.7 Compute the expectation

Once the coefficients of the piecewise polynomials have been calculated, to obtain an explicit expression for the integral form of the expected volatility, Equation 1, we compute by using the approximated function gained from interpolating the selected options data:

$$\int_{-\infty}^{\infty} \sigma^2(d_2)\phi(d_2)dd_2 \approx \sum_i \int_{x_i}^{x_{i+1}} y_i(x)\phi(x)dx + \int_{x_{\max}}^{\infty} a_{\max}\phi(x)dx + \int_{-\infty}^{x_0} a_0\phi(x)dx$$

By making repeated use of the fact $\frac{d}{dx}\phi(x) = -x\phi(x)$ when integrating by parts we obtain the following equations,

$$\int_{x_i}^{x_{i+1}} y_i(x)\phi(x)dx = a_i A_i + b_i Bi + c_i C_i + d_i D_i$$

$$A_i = \Phi(x_{i+1}) - \Phi(x_i)$$
$$B_i = \phi(x_i) - \phi(x_{i+1}) - A_i \cdot x_i$$
$$C_i = (1 + x_i^2) \cdot A_i - 2x_i \cdot (\phi(x_i) - \phi(x_{i+1})) + x_i \cdot \phi(x_{i+1}) - x_{i+1} \cdot \phi(x_{i+1})$$
$$D_i = (x_{i+1}^2 + 2) \cdot \phi(x_i) + (3x_i x_{i+1} - 3x_i^2 - x_{i+1}^2 - 2) \cdot \phi(x_{i+1}) - x_i(3 + x_i^2) \cdot A_i$$

As the tails in this case are constant extrapolations, they are dealt with as follows:

$$\int_{x_{\max}}^{\infty} a_{\max}\phi(x)dx = a_{\max}(1 - \Phi(x_{\max}))$$

And similarly for the lower tail.

4 Summary of Testing Methods

We focus on computing and comparing the Quadratic Variation (QV) obtained from the following four methods:

1. **True QV**: The benchmark volatility measure, calculated from realized historical returns. Specifically, we use the annualized realized variance(5-min) provided by the Oxford-Man Realized Volatility dataset for SPX[Oxf]. These values serve as the baseline for evaluating the error of other QV estimation methods under real market conditions. We focus on two time periods: the years 2008 and 2018, which represent high-volatility and low-volatility regimes respectively

2. **Paper QV**: The method proposed in the paper and detailed in section 3.1. The key features are the use of a C^1 cubic spline interpolation of $\sigma(d_2)$ with flat extrapolation.

3. **CBOE QV**: The industry-standard method based on the CBOE VIX formula. We implement the discrete approximation of the VIX calculation:

   (i) using available option prices, compute the weighted sum of call and put option prices across strikes;

   (ii) apply the discrete formula from the CBOE whitepaper to estimate the implied variance.

4. **Natural Cubic QV (Natural QV)**: Inspired by the interpolation method proposed by Tian et al[JT07], but not directly applicable as we work on the function $\sigma(d_2)$ as opposed to $\sigma(k)$. This approach involves the computation of natural cubic splines, C^2 with second derivative zero at the end points, with a linear extrapolation at the end points. As $\sigma(d_2)$ need only be C^1 and this approach is C^2, it is too specific, but allows for comparison of the change to linear extrapolation with the original method.

5. **Quadratic QV (Quad QV)**: Based on the method described in the paper, but instead making use of quadratic splines, matching gradients except at the left end point, with flat extrapolation. The result is a C^1 function except at the left end point, where it remains continuous. This method was selected to demonstrate why it is necessary to include the additional freedom of cubic splines over quadratic.

6. **Clamped Cubic QV (Clamp QV)**: An alternative version of Paper QV that replaces their cubic spline interpolation with a clamped C^2 interpolation, with flat extrapolation. $d_2 \to \sigma$ mapping.

5 Testing on Simulated Data

We will now test the algorithm provided in the paper on simulated data to test how well it in this environment. Like the paper, we are going to simulate the data using a Heston model. This model is defined as,

$$dS_t = S_t\sqrt{V_t}[\rho dW_t^1 + \sqrt{1-\rho^2}dW_t^2],$$
$$dV_t = \lambda(\upsilon - V_t)dt + \eta\sqrt{V_t}dW_t^1.$$

Parameter Set	λ	υ	η	ρ	V_0
A	1.0	0.2	0.5	-0.8	0.6
B	1.0	0.2	1.0	-0.4	0.6
C	5.0	0.04	1.0	-0.4	0.6
D	1.5	0.04	0.3	-0.7	0.04

Table 1: Values of Heston model variables under different parameter sets.

Here, (W_t^1, W_t^2) represent a two dimensional Brownian motion. The parameters used can be seen in Table 1. We generate the theoretical option prices by using a Monte Carlo simulation. We then generate the bid and ask prices using a similar procedure from the paper. We use a geometric random variable with $p = 0.8$ to calculate how many ticks above (below) the theoretical price the ask (bid) price is. Using this procedure we can very easily compare the different methods of calculating the QV since the expected true QV can be analytically calculated. The expected true QV under a Heston model is [Gat06, p.138],

$$\upsilon + \frac{1-e^{-\lambda T}}{\lambda T}(V_0 - \upsilon).$$

Parameter Set	True QV	CBOE QV	Paper QV	Natural QV	Quad QV	Clamp QV
A	0.5816	0.4594	0.5669	0.5676	0.5701	0.5668
B	0.5816	0.4561	0.5563	0.5201	0.5566	0.5560
C	0.4856	0.3954	0.4759	0.4778	0.4781	0.4762
D	0.0400	0.0428	0.0401	0.0383	0.0399	0.0401

Table 2: Estimated QV for different methods for different parameter sets, under $T = 0.0952$ as in the paper.

Parameter Set	True QV	CBOE QV	Paper QV	Natural QV	Quad QV	Clamp QV
A	0.5675	0.4039	0.5490	0.6766	0.5488	0.5490
B	0.5675	0.4035	0.5441	0.5689	0.5441	0.5441
C	0.4157	0.3096	0.4004	0.4532	0.4010	0.4004
D	0.0400	0.0401	0.0394	0.0382	0.0394	0.0394

Table 3: Estimated QV for different methods for different parameter sets, under $T = 0.1719$ as in the paper.

Tables 2 and 3 display the QV estimates under these simulations for $T = 0.0952$ and $T = 0.1719$ respectively. These values of T, and the parameter sets were chosen to recreate the results from the paper. In particular A, B, and C are meant to represent stressed market conditions, with D representative of more normal market conditions. We notice that the QV estimates from the method in the paper are consistently closer to the true QV compared to the CBOE method's QV. The CBOE's QV only performs better under parameter set D when $T = 0.1719$, however considering the paper method's QV is very close this does not seem significant, and is expected as parameter set D is designed to replicate normal market conditions. We also notice that the Natural QV tends to perform worse than the paper's method, however there are a few occurrences where it outperforms the paper's method.

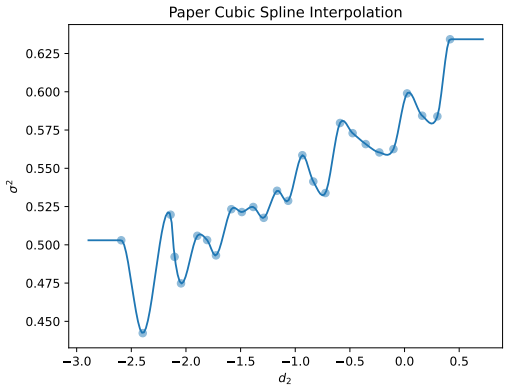

(a) Paper Interpolated Polynomial for Set A.

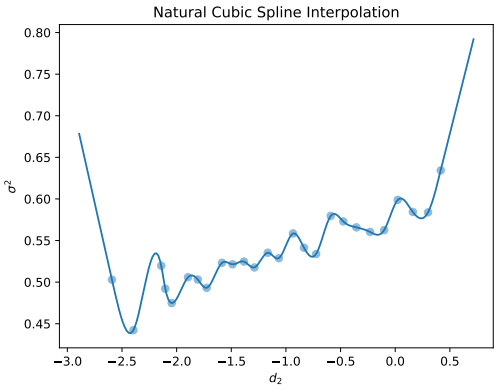

(b) Natural Interpolated Polynomial for Set A

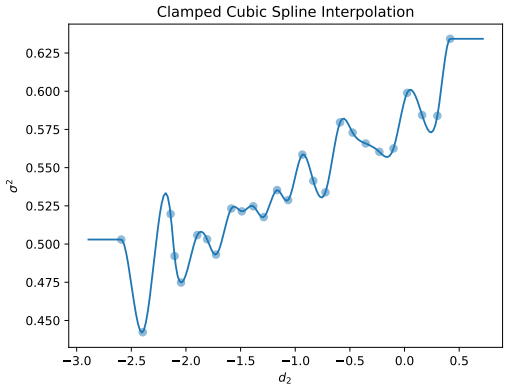

(c) Clamped Interpolated Polynomial for Set A.

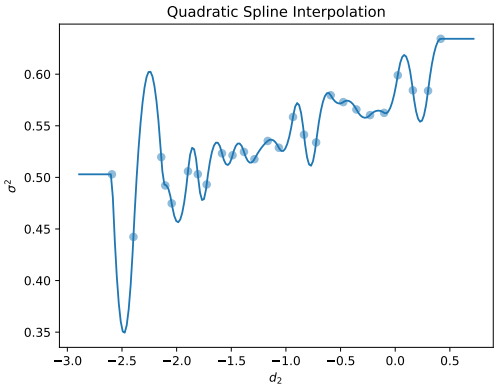

(d) Quadratic Interpolated Polynomial for Set A.

Figure 1: Plots for the different methods under one sample of parameter set A.

This is likely due to the linear extrapolation, as can be observed in Figure 1b.

We also notice that the quadratic method's QV and clamped method's QV generally do not outperform the paper method's QV. However, since these methods are very similar in extrapolation to the paper's method, their QV is very close to that of the paper method's QV. There are signs from Figure 1d that our Quadratic interpolation method suffers from potential large oscillations, which could cause large errors on rougher data.

6 Testing on Real Data

In this section, we apply real market data to empirically test the model-free implied volatility estimation method proposed in the paper. The dataset is sourced from **OptionMetrics SPX option data**, covering the year from 2008 to 2018. By testing on real data, we aim to validate the effectiveness of the paper's method under actual market conditions, and compare it against several approaches for expected volatility/quadratic variation (QV) estimation.

6.1 Data Preparation

Prior to computation, we performed data cleaning to ensure the reliability of our results:

- Selected SPX option data from the year 2008 to 2018;
- Filtered out illiquid options with missing bid-ask quotes or zero volume;

- Matched call and put options for each day to ensure completeness;
- Used the bisection method to compute implied volatilities from option prices;
- Prepared required inputs for Paper QV, Natural QV, Quad QV, and Clamp QV, including implied volatilities, d_2 values, and interpolation curves.
- To ensure consistency in comparison and reduce noise due to varying option maturities, we focus on options with 30 days and 10 days to maturity. Since each date may have multiple available expiries. This allows us to estimate the expected QV over a fixed horizon and compare it with the realized True QV on the corresponding expiry date.

6.2 Results

6.2.1 Comparison of Quadratic Variation across Methods

To begin, we present a sample of the computed Quadratic Variation (QV) values for each method, based on real SPX option data in 2008-2018, 30 days and 10 days to maturity.

Date	Exdate	True QV	CBOE QV	Paper QV	Natural QV	Quad QV	Clamp QV
2008-12-01	2008-12-31	0.037642	0.122305	0.047950	0.005234	0.120682	0.005607
2009-08-31	2009-09-30	0.039591	0.017060	0.024141	-0.003522	-0.047166	-0.003455
2009-12-01	2009-12-31	0.005066	0.014356	0.021654	-0.001934	0.072748	-0.002197
2010-03-01	2010-03-31	0.011322	0.010573	0.017397	-0.009601	-0.074568	-0.009574
2010-08-31	2010-09-30	0.033635	0.019576	0.024301	-0.002818	0.122548	-0.003606
⋮	⋮	⋮	⋮	⋮	⋮	⋮	⋮
2018-04-23	2018-05-23	0.007416	0.006854	0.011490	0.009146	0.038007	0.009154
2018-04-25	2018-05-25	0.004211	0.008714	0.013206	0.010928	0.345469	0.010878
2018-04-30	2018-05-30	0.005519	0.006180	0.010980	0.008601	0.120646	0.008600
2018-05-01	2018-05-31	0.010408	0.006123	0.010792	0.008361	0.256625	0.008381
2018-05-02	2018-06-01	0.005225	0.006523	0.011287	0.008873	0.238071	0.008891

Table 4: Sample QV values from each method, 30-Day Maturity, 2008-2018

Date	Exdate	True QV	CBOE QV	Paper QV	Natural QV	Quad QV	Clamp QV
2008-06-20	2008-06-30	0.022807	0.013387	0.043770	0.002949	0.505539	0.016510
2009-12-21	2009-12-31	0.005066	0.009596	0.078100	-0.060205	5.112888	-0.059602
2010-09-20	2010-09-30	0.033635	0.011463	0.039190	0.004571	0.137299	0.004566
2010-12-21	2010-12-31	0.002481	0.006066	0.028882	0.002511	1.008834	0.002535
2011-03-21	2011-03-31	0.004433	0.011982	0.041295	0.013497	-0.817895	0.013629
⋮	⋮	⋮	⋮	⋮	⋮	⋮	⋮
2018-04-17	2018-04-27	0.008709	0.006825	0.030192	0.016982	1.046348	0.017039
2018-04-20	2018-04-30	0.012078	0.006437	0.033040	0.019888	-0.522019	0.019947
2018-04-24	2018-05-04	0.011606	0.010485	0.042913	0.029786	0.009117	0.029849
2018-04-27	2018-05-07	0.007152	0.004750	0.027042	0.013399	2.042497	0.013355
2018-05-01	2018-05-11	0.005361	0.006894	0.033360	0.019602	2.693990	0.019694

Table 5: Sample QV values from each method, 10-Day Maturity, 2008-2018

To compare the behavior of different QV methods, we first calculate the sample means of each estimator under 30-day and 10-day maturities. The results are presented in Table 6. Substantial differences in the average QV values reflect fundamental differences in model construction.

For the 30-day maturity, CBOE QV, Paper QV, Natural QV, and Clamp QV all produce estimates lower than the benchmark True QV. Among them, Paper QV is the closest to True QV, indicating

QV Method	Mean
True QV	0.012695
CBOE QV	0.008222
Paper QV	0.011949
Natural QV	0.006761
Quad QV	0.047270
Clamp QV	0.006773

30-Day Maturity

QV Method	Mean
True QV	0.014702
CBOE QV	0.008087
Paper QV	0.033987
Natural QV	0.013859
Quad QV	0.076822
Clamp QV	0.013969

10-Day Maturity

Table 6: Mean of QV Measures Across Different Maturities

relatively good performance. In contrast, Quad QV significantly overestimates the benchmark, suggesting a tendency toward systematic inflation.

However, under the 10-day maturity, the mean of Paper QV increases drastically to 0.033987, far above the True QV and all other methods. This sharp deviation suggests that the Paper method may suffer from instability in short-term settings, likely due to structural limitations in its algorithm. We will discuss this issue further in a later section.

Overall, Clamp QV and Natural QV remain relatively stable across both maturities, maintaining consistent proximity to the benchmark. CBOE QV persistently underestimates True QV, but the deviation is moderate and consistent.

In summary, Paper QV performs best at the 30-day horizon, but its large upward bias at 10 days highlights potential limitations in robustness.

6.2.2 Time Series Comparison of QV Estimates

To further investigate the dynamic performance of each QV estimation method, we replicate the time series comparison plots presented in the original paper.

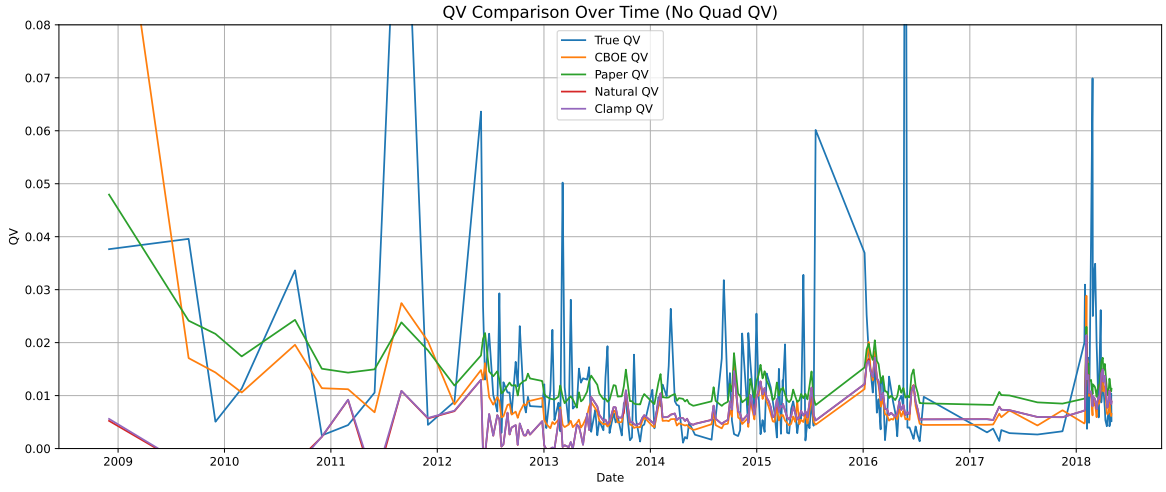

Figure 2: Time series comparison of QV estimates from different methods, 30-Day Maturity

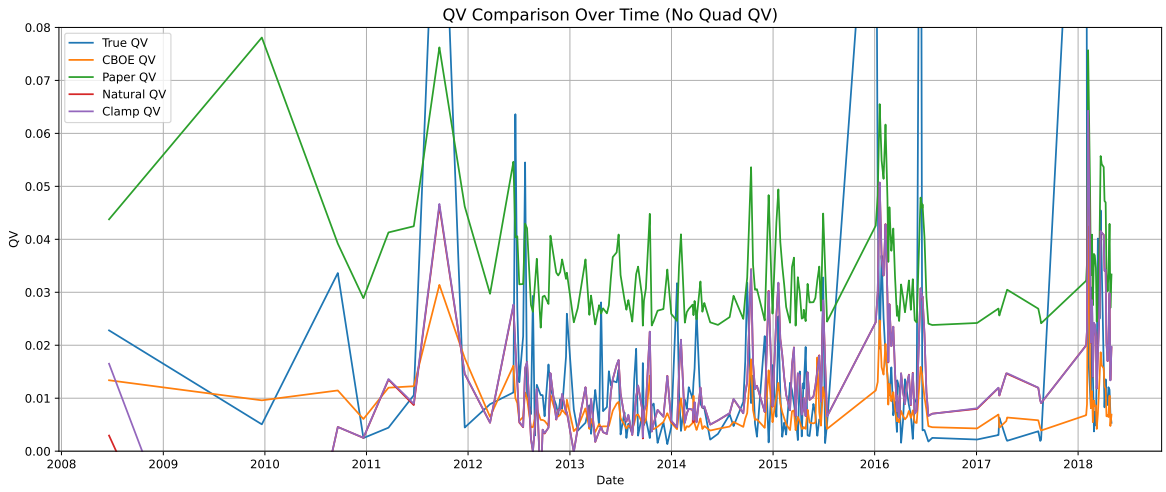

Figure 3: Time series comparison of QV estimates from different methods, 10-Day Maturity

Figures 2 and 3 illustrate the time series behavior of various QV estimation methods over the period 2008–2018, for 30-day and 10-day maturities, respectively. These plots offer additional insights into the temporal dynamics beyond average-level comparisons.

First, we observe that Paper QV exhibits significant volatility and pronounced spikes, particularly between 2011 and 2013. These upward deviations frequently overshoot the True QV benchmark, especially for the 10-day maturity case. Such patterns suggest instability in the algorithm under shorter-term maturities.

In contrast, both Natural QV and Clamp QV maintain smoother trajectories and closely track the movement of True QV throughout most of the sample period. Their stability is especially evident in post-2015 periods of moderate market volatility, where the curves almost coincide with the True QV line.

CBOE QV appears to consistently overestimate QV during the early years 2008–2010, possibly due to higher implied volatility premiums or illiquidity in option markets during the financial crisis. However, its estimates become more aligned with the True QV in the latter years, suggesting improved market efficiency or better calibration.

Quad QV is excluded from the figures due to its extremely erratic behavior, as reflected in the earlier summary statistics. This further supports its unsuitability for direct visual comparison.

Finally, when comparing the two maturities, it becomes evident that shorter horizons 10-day lead to increased instability and estimation errors across all methods. Volatility clustering and market shocks, amplify the divergence from the True QV, underscoring the greater sensitivity of short-maturity estimates to noise and model specification.

These visual results complement the previous mean analysis and highlight the importance of evaluating both point accuracy and temporal robustness when comparing QV estimation techniques.

6.2.3 Error-Based Evaluation: RMSE and MAE

To further quantify the accuracy of each method, we compute the Root Mean Squared Error (RMSE) and Mean Absolute Error (MAE) between each method's QV estimates and the True QV benchmark. These metrics allow us to evaluate both average accuracy and sensitivity to larger deviations.

Method	RMSE	MAE
CBOE QV	0.018599	0.008521
Paper QV	0.017076	0.008672
Natural QV	0.018856	0.009189
Quad QV	0.436374	0.195044
Clamp QV	0.018857	0.009183

30-Day Maturity

Method	RMSE	MAE
CBOE QV	0.022616	0.009773
Paper QV	0.029060	0.024363
Natural QV	0.022393	0.012084
Quad QV	1.278181	0.774091
Clamp QV	0.022331	0.012001

10-Day Maturity

Table 7: RMSE and MAE of each method against the True QV benchmark

Table 7 reports the Root Mean Squared Error (RMSE) and Mean Absolute Error (MAE) of each QV estimation method compared to the True QV benchmark. These metrics provide a quantitative evaluation of the estimation accuracy under both 30-day and 10-day maturities.

We observe that overall error levels are lower for the 30-day maturity compared to the 10-day, suggesting that a longer horizon improves estimation stability. Under the 30-day maturity, Paper QV achieves the lowest RMSE and MAE values, slightly outperforming Natural QV and Clamp QV. This confirms Paper QV's strong fitting performance over monthly cycles, despite occasional spikes observed in the time series plots. In contrast, Quad QV shows significantly higher errors, indicating poor numerical behavior and model misalignment. This method is clearly unsuitable in our framework.

Under the 10-day maturity, the performance of Paper QV deteriorates notably, with its RMSE rising to 0.029060 and MAE to 0.024363. Its ranking falls behind CBOE, Natural, and Clamp QV, suggesting instability or over-sensitivity in its algorithm when applied to high-frequency estimates. We hypothesize that this is due to interpolation weights or smoothing schemes that become unstable for shorter maturities, which we will explore further in later sections.

Importantly, both Clamp QV and Natural QV maintain robust performance across maturities, indicating their consistency and reliability in varying market conditions. CBOE QV, while simple and intuitive, exhibits slightly higher errors and some volatility, especially under the 10-day maturity.

In summary, Quad QV should be excluded due to its poor accuracy. Paper QV is promising for longer horizons but problematic in the short term. Natural QV and Clamp QV are the most robust estimators across both settings, but the original CBOE method appears to be the most robust of all.

6.3 Discussion on the Natural QV Method

In our empirical analysis for 30-Day Maturity, the performance of the Natural QV method falls within the expected range. Although it achieves acceptable results in certain samples, its overall error remains higher than that of the Paper QV. Given the structural limitations of the Natural QV approach in handling tail implied volatilities, we further developed two alternative strategies: Clamp QV and Quad QV. Clamp QV is intended to be similar to Natural QV in its interpolation scheme, being C^2, only differing in the use of constant extrapolation as opposed to the linear extrapolation in the natural approach. Quadratic QV is instead intended to compare reduction in the degrees of freedom in interpolation, through the use of quadratic splines, whilst otherwise using constant extrapolation.

The Paper method, informed by the work of Jiang and Tian (2005) [JT07], which violated no arbitrage conditions with a *linear extrapolation* of $\sigma(k)$, instead employs *flat extrapolation* to extend the implied volatility surface at extreme strikes. However in real markets, volatility smiles or skews typically cause implied volatilities to rise as the strike moves away from the money. Flat extrapolation neglects this trend, potentially leading to systematic underestimation and thus lower QV estimates. Natural QV, which instead implements a linear extrapolation of $\sigma(d_2)$ (not of $\sigma(k)$ and therefore not necessarily violating no arbitrage conditions) allows comparison of alternative extrapolation.

Clamp QV and Natural QV deliver comparable results at the 30-day maturity, both outperforming the CBOE QV and showing relatively stable behavior. However, their performance deteriorates in the

10-day case, with noticeable increases in error. Notably, Clamp QV serves as a partial substitute when Paper QV under-performs.

The CBOE QV method tends to systematically underestimate volatility across both maturities, likely due to its lack of sensitivity to extreme strikes, due to the truncation of the integral in the derivation of the approximation.

Overall, Paper QV performs best at the 30-day maturity, balancing high accuracy and smoothness. Estimates closely track the True QV. Nevertheless, at the 10-day maturity, Paper QV suffers from a significant loss of accuracy and increased instability, suggesting structural limitations of its extrapolation scheme in short-term settings.

In conclusion, while our proposed alternatives Clamp QV and Quad QV offer certain improvements in stability, Paper QV remains the most effective method at longer maturities. The increased estimation error across all methods at shorter maturities highlights the need for more robust extrapolation techniques specifically tailored to short-term options.

7 Key Aspects of the Methodology

The main difference between the paper's methodology and the CBOE procedure, apart from the alternative formulation of the integral, is the lack of truncation of the integral estimating the expected quadratic variation. The CBOE method discards the contribution to the integral outside of the available strike range $[K_{min}, K_{max}]$. Reparameterising the integral to the paper's formulation, and based on the monotonicity of d_2, it discards the contribution to the integral from beyond the maximum and minimum d_2. In normal market conditions, this truncation is not necessarily a problem, as seen in simulated data set D in Tables 2 and 3, or in the real world data seen in Table 4.

Examining this more closely, in Figure 4a we note that the real world data d_2 for which the option data spans is from -4 to around 3.7, and so the contribution from the tails is very minor, due to the small tails of $\phi(x)$. Therefore truncation does not have a significant impact on the calculation.

Data set A is designed to represent more stressed market conditions, as per the original paper [FIM+11]. This allows for comparison. We see that in simulated data for data set A as seen in Figure 1a, that d_2 instead spans from -2.6 to 0.4. So the contribution from $\phi(x)$ from 0.4 and above is significant. The truncation of the CBOE procedure, especially at the upper range where σ^2 is around 0.625 results in significant underestimation of the expected quadratic variation.

Therefore one of the key elements the paper corrects for is the truncation inherent in the CBOE procedure, by a constant flat extrapolation of $\sigma^2(d_2)$. Although this is still likely an underestimate of the overall quadratic variation (depending on the distribution of the data), it performs significantly better in the stressed simulated market conditions, A, B and C, as seen in Tables 2 and 3.

Finally the other key aspect of the methodology is the choice of interpolation. As can be seen in Figure 4 the choice of the paper's method of C^1 cubic interpolation, rather than a C^2 interpolation, results in undesirable oscillations to be suppressed. Specifically we see that the paper's interpolation of the 2014-01-08 data results in smaller negative values of σ^2 compared to a C^2 clamped interpolation.

This can also be seen in Figure 1, where especially around $d_2 = -2.2$ significant overshoot can be seen in both of the C^2 cubic interpolations, and very significantly in the quadratic C^1 interpolation. In the real world data, these oscillations clearly cause poor performance, as is especially noted in the Quadratic interpolation results seen in Tables 5 and 4.

8 Paper Critiques

8.1 Calculation of at the money Forward Price

In calculation of the at the money forward price, there is no consideration of whether data may be stale, which could distort the algorithm somewhat. A possible improvement to the algorithm could be to ensure a time cut-off to ensure only recent transactions are used so the data is not stale when calculating the at the money price.

An alternative method could simply be to use the market forward price, and then choose the strike which gives the closest value under put-call parity as the implied strike.

8.2 Clean Options Data Selection Ratio

The choice to discard all options where the ask price is 2 or more times the bid price seems arbitrary. Specifically in the choice of 2, as well as this method for choosing reliable data.

There may be a better way of selecting suitable, up-to-date options data based on how recent the bid/ask transactions were for the particular option, which may ensure more reliable data.

8.3 Calculation of Implied Volatility

The paper makes use of a bisection algorithm in order to calculate the implied volatilities for each option. However, better methods for root finding exist that converge faster. An example would be the Newton Raphson method, which would be suitable in this case.

8.4 Choice of Constant Extrapolation

In the paper, "Extracting model-free volatility from option prices: An examination of the VIX index." by Jiang and Tian [JT07] is cited as an alternative method of improving the CBOE procedure. The Tian model instead attempts to fit the implied volatilities, σ, as a function of k using cubic splines ensuring the resulting surface is C^2 (twice differentiable), and then proceeds via numerical integration. This differs from the method proposed here, in which σ is treated instead as a function of d_2 for polynomial interpolation. One of the criticisms leveled at the Tian technique is that, outside of the range of observed data points, a linear extrapolation is used. While this does in fact violate $\sigma(k) < \sqrt{2k}$, and so is a valid criticism of the Tian paper, it is not directly applicable to the technique proposed in the Fukasawa et al paper [FIM+11], where it is used to rule out a linear extrapolation scheme for $\sigma(d_2)$. Taking $\sigma(k) \approx A\sqrt{k}$ for large k, we find that after substituting into the equation for d_2, Equation 7

$$\sigma(d_2) \approx -\frac{2A^2\sqrt{T}}{2 + A^2 T} d_2$$

Which is linear in d_2. So in fact a quadratic extrapolation should not be ruled out for $\sigma^2(d_2)$, so long as the rate of growth is controlled.

A clear example would be in the real data as seen in Figure 4 where an abrupt constant extrapolation does not appear to fit the data well.

8.5 Choice of Cubic Splines

The paper makes use of Cubic splines, a C^1 approximation, where because of the extra degree of freedom the gradients are chosen such that the gradients of adjacent points are such that the angle of incidence is equal to the angle of reflection in the horizontal plane to the x axis where the gradients intersect.

However, it is not immediately clear what motivates such a choice. Whatever extension is used, it must be C^1. d_2 is a monotonic and smooth function of k (since $\sigma(k)$ is at least C^1). Choosing an extrapolation scheme that has a kink at the join point therefore also implies that $\sigma(k)$ will have a discontinuity in its derivative. As noted in the paper by Tian and Jiang [JT07] this implies that the local risk neutral density is negative, violating no arbitrage conditions in the volatility surface. In the case of the paper by Fukasawa et.al [FIM+11] it is imposed that the extrapolation is flat. Therefore we also know the start and end gradients.

Therefore matching the start and end gradients, combined with the gradient reflection principle allows for all of the coefficients of the cubic splines to be computed. However it's not clear why this method of gradient matching is used, and the paper does not motivate this choice. It is possible a more general or motivated method of interpolation exists.

8.6 Model Evaluation Method

When evaluating the performance of the paper's method and the original CBOE method on real data, the paper suggests using the R^2 of the following linear regression to evaluate performance:

$$\hat{V}_t = \alpha + \beta\, IV_t + u_t$$

where $\hat{V}$ and IV represent the annualized realized variance and implied variance respectively.

However this method is not well motivated in the paper, with u_t undefined, and it is not clear to us why a simple comparison of $\hat{V}$ and IV via root mean squared error, and mean absolute error is not used, which is the case in our own statistics.

8.7 Volatility Surfaces with Negative Volatility

As a result of the interpolation method, it is possible for the interpolated volatility function $\sigma(d_2)$ to be negative at points, especially where there is a single strike with very small volatility.

This issue is less significant in the paper's method when compared to the extensions. An example is displayed in Figure 4, where both the clamped method and the paper's method exhibit negative volatility in their interpolations. However, this is significantly less pronounced in the paper's method (and is barely noticeable in the graph).

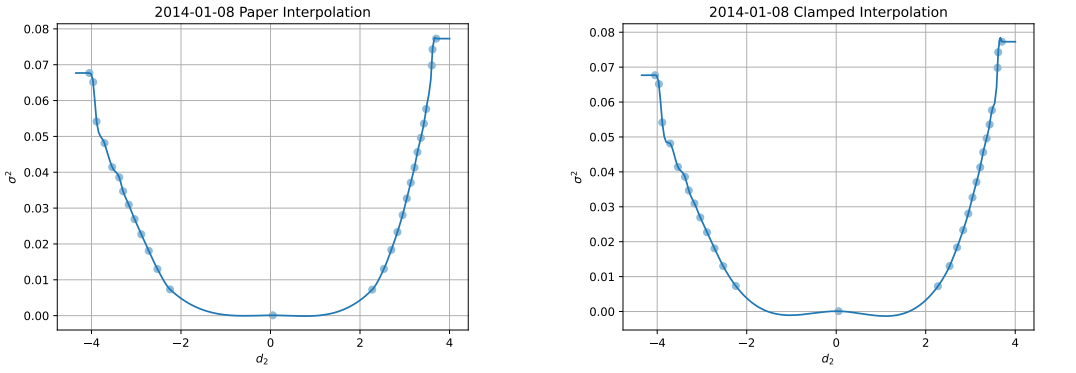

(a) 2014-01-08 Paper Interpolated Function (b) 2014-01-08 Clamped Interpolated Function

Figure 4: Comparison of Paper vs. Clamped Interpolated Functions on 2014-01-08

9 Extensions

9.1 Implemented Extensions

9.1.1 C^2 Cubic Splines

Informed by the Tian and Jiang [JT07] method of interpolating $\sigma(k)$ we proceed in the same way in interpolating $\sigma^2(d_2)$. We added in a model which instead fits with 'natural' cubic splines, designed to ensure that the resultant function is C^2 everywhere in the interior of valid points, and smooth at the end points. However this method of choosing cubic splines results in us having no further freedom over the choice of any of the other parameters. We are forced to take a linear extrapolation at the end points in order to ensure that the overall function is C^1, which can result in poor performance depending on the gradient of the required extrapolations. In this case we made use of the Scipy Python package CubicSpline, with 'natural' spline parameters to find the parameters a_i, b_i, c_i, d_i for each of the data points $d_2(k_i)$.

For completeness, we also make use of 'clamped' cubic splines, where instead the gradient at the end is forced to be zero, in combination with constant extrapolation for comparison against the method, again making use of the Scipy Python package to compute the polynomial coefficients.

9.1.2 Quadratic Splines

Given that the resulting function of $\sigma^2(d_2)$ is only required to be C_1, we also fitted the data with quadratic splines, while also demanding constant extrapolations. This will not be a valid volatility surface as a result of the discontinuity in the derivative at the extension, however is used for comparison, to show that the main benefit of the paper's method is in the choice of constant extrapolation, and explicit evaluation of the integral expression 2, rather than obtaining a good interpolation that exactly matches the already obtained implied volatility data.

By matching the gradients at both ends of the intervals, the following equations can be derived with Δx_j and Δy_j as before.

$$
\begin{aligned}
a_j &= y_j, \\
b_j &= \frac{2\Delta y_j - b_{j+1}\Delta x_j}{\Delta x_j} \\
c_j &= \frac{\Delta y_j - b_j \Delta x_j}{\Delta x_j^2}
\end{aligned}
$$

This choice of interpolation allows us freedom to choose the gradient at either x_0 or $x_{\max}$. We choose this to be flat at $x_{\max}$ to match the flat extrapolation, however we may end up having a kink at the beginning, violating no arbitrage conditions as a result.

9.2 Additional Extensions

9.2.1 Implement Tian Method

As the paper mentions the Tian and Jiang [JT07] method of computing the expected volatility for critique and comparison to its own method, a possible extension could implement the Tian method based on interpolating and numerically integrating $\sigma^2(k)$ and then comparing to the paper method.

9.2.2 Different Tail Extrapolation

As noted in our criticisms in Section 8.4, quadratic tail growth of $\sigma^2(d_2)$ does not necessarily violate no arbitrage conditions. Therefore a possible extension could be to investigate whether alternative extrapolation schemes for the tails of the approximated function are more appropriate.

9.2.3 Alternative fit

As many of the simulated data point graphs appear to have large oscillations in the observed values 1a, if we abandon the requirement to fit exactly the observed data with our curve, and instead fit a calibrated curve to $\sigma^2(d_2)$, we can integrate this directly using the key model free formula 2, which may provide more robust performance.

9.2.4 Alternative interpolation

An alternative interpolation scheme could be implemented. Specifically one which excludes the possibility of negative volatility values to avoid the issue noted in section 8.7

10 Conclusions

Overall, of the interpolation approaches the Paper QV method demonstrates the most robust performance on real market data, delivering the lowest RMSE and MAE among all approaches. This confirms the effectiveness of its smooth mapping from $d_2 \to \sigma$, particularly highlighting the impact of interpolation method choice. The choice of interpolation reduces the possibility of wild oscillations and large negative values in the approximated function. Notably, the Paper QV outperforms the Clamp QV approach for this reason, even though the only difference lies in adopting a C^2 cubic spline interpolation instead of a basic constant extension.

Regarding the Natural QV method, although it adopts linear extrapolation at the tails of the volatility surface. This can lead to overestimation in high-volatility regions. Empirically, its error is close to Clamp QV, indicating that the method remains relatively stable when the extrapolation region is limited, as is expected in typical market data and the volatility surface behaves smoothly.

Quadratic interpolation, although C^1 except at the left end point, does not provide good performance. The interpolation is too restrictive and leads to large oscillations on real world data resulting in poor performance including predictions of negative volatility.

The performance on simulated data shows that the CBOE method fails to perform in times of market stress, where the volatility surface is significantly skewed. Because of tail truncation in the CBOE method, it systematically underestimates volatility in these cases.

These findings highlight the critical importance of robust tail modeling in model-free QV estimation. Even with theoretical guarantees, the structure of the extrapolation, the availability of tail option data, and the interpolation technique can substantially affect final estimation accuracy.

However on real data, especially on shorter maturities, our implementation of the paper method appears to suffer from systematic overestimation of the estimated volatility. The CBOE method does not suffer from this, and therefore may be more robust on more standard market data where the tail extrapolation is not important.

In summary, the Paper QV method remains an accurate and consistent approach in our empirical study, validating its theoretical framework and practical effectiveness, but may suffer from instability on shorter maturities.

References

[BL78] Douglas T Breeden and Robert H Litzenberger. Prices of State-Contingent claims implicit in option prices. *The Journal of Business*, 51(4):621–651, 1978.

[FIM+11] M. FUKASAWA, I. ISHIDA, N. MAGHREBI, K. OYA, M. UBUKATA, and K. YAMAZAKI. Model-free implied volatility: From surface to index. *International Journal of Theoretical and Applied Finance*, 14(04):433–463, 2011.

[Gat06] Jim Gatheral. *The Volatility Surface: A Practitioner's Guide." The Volatility Surface*, volume 357. John Wiley & Sons, United States, 2006.

[JT07] George Jiang and Yisong Sam Tian. Extracting model-free volatility from option prices: An examination of the vix index. *Journal of Derivatives, Vol. 14, No. 3*, 2007.

[Lee04] Roger Lee. The moment formula for implied volatility at extreme strikes. *Mathematical Finance*, 14:469–480, 02 2004.

[Oxf] Oxford-Man Institute's Realized Library, version 0.3., now discontinued.

A Proof of lemmas

For these proofs we will again follow the style of the paper [FIM+11].

A.1 Proof of Lemma 1

Firstly, we define the following quantity,

$$D_{BS}(K) := \frac{dP_{BS}}{dK}(\log(\frac{K}{F}), \Sigma)|_{\Sigma=\sigma(\log(\frac{K}{F}))} = \Phi(-d_2(k, \sigma(k))).$$

The second equality is due to simple differentiation of the put value. Then we notice that,

$$\begin{aligned}
D(K) &= \frac{dP}{dK}(K), \\
&= \frac{d}{dK} P_{BS}\left(\log\left(\frac{K}{F}\right), \sigma\left(\log\left(\frac{K}{F}\right)\right)\right), \\
&= D_{BS}(K) + \frac{1}{K}\frac{\partial P_{BS}}{\partial \Sigma}\left(\log\left(\frac{K}{F}\right), \sigma\left(\log\left(\frac{K}{F}\right)\right)\right)\frac{d\sigma}{dk}\left(\log\left(\frac{K}{F}\right)\right), \\
&= D_{BS}(K) + \phi\left(-d_2\left(\log\left(\frac{K}{F}\right), \sigma\left(\log\left(\frac{K}{F}\right)\right)\right)\right)\frac{d\sigma}{dk}\left(\log\left(\frac{K}{F}\right)\right).
\end{aligned}$$

The last line follows from the known derivative of Black-Scholes put with regard to the volatility (vega).

A.2 Proof of Lemma 2

We begin by defining,

$$f(k) := -d_2(k, \sigma(k)) = \frac{k}{\sigma(k)} + \frac{\sigma(k)}{2}.$$

Here we have omitted $\sqrt{T}$, as we have discussed previously. From simple differentiation, we get the result,

$$\begin{aligned}
\frac{df}{dk}(k) &= \frac{1}{\sigma(k)} - \frac{d\sigma}{dk}(k)\frac{k}{\sigma(k)^2} + \frac{1}{2}\frac{d\sigma}{dk}(k), \\
&= \frac{1}{\sigma(k)}\left\{1 - \frac{d\sigma}{dk}(k) f(k)\right\} + \frac{d\sigma}{dk}(k).
\end{aligned}$$

Using the fact that,

$$-d_2(k, \sigma(k))\frac{d\sigma}{dk}(k) < 1, \tag{8}$$

for all $k \in \mathbb{R}$, we now get the result,

$$\frac{df}{dk}(k) > \frac{d\sigma}{dk}(k).$$

This means that we only need to consider the case where $\frac{d\sigma}{dk}$ is less than 0, since when this is larger than 0, so must $\frac{df}{dk}$. Equation 8 is proven as a Lemma in the paper[FIM+11], however we do not prove it here due to the limited space for this coursework. Then, using the fact that,

$$-f(k) + \sigma(k) = d_1(k, \sigma(k)),$$

we get that,

$$\frac{df}{dk}(k) = \frac{1}{\sigma(k)} \left\{ 1 + \frac{d\sigma}{dk}(k) d_1(k, \sigma(k)) \right\}.$$

Now, if $d_1(k, \sigma(k)) < 0$ and $\frac{d\sigma}{dk} < 0$, we must have that $\frac{df}{dk} > 0$, proving the result in this case. The only case we now need to consider is when $d_1(k, \sigma(k)) \geq 0$ and $\frac{d\sigma}{dk} < 0$. For this case we will prove the result that for all k with $d_1(k, \sigma(k)) \geq 0$,

$$d_1(k, \sigma(k)) \frac{d\sigma}{dk}(k) > -1. \tag{9}$$

We begin by stating that for $K > 0$,

$$KD(K) \geq P(K).$$

Then using Lemma 1 with this result and the known formulae for $P(K)$, we get the result,

$$F\Phi(-d_1(k, \sigma(k))) + K\phi(-d_2(k, \sigma(k))) \frac{d\sigma}{dk}(k) \geq 0.$$

We now notice that,

$$\begin{aligned}
K\phi(-d_2) &= K \frac{1}{\sqrt{2\pi}} \exp(-\frac{(-d_2)^2}{2}), \\
&= K \frac{1}{\sqrt{2\pi}} \exp(-\frac{(\sigma - d_1)^2}{2}), \\
&= K\phi(-d_1) \exp(-\frac{1}{2}\sigma^2 + d_1\sigma), \\
&= K\phi(-d_1) \exp(-\frac{1}{2}\sigma^2 + \frac{1}{2}\sigma^2 - k), \\
&= F\phi(-d_1).
\end{aligned}$$

Substituting this relation into the previous result gives us,

$$\frac{d\sigma}{dk}(k) \geq -\frac{1 - \Phi(d_1(k, \sigma(k)))}{\phi(d_1(k, \sigma(k)))}.$$

Finally, we use the known result,

$$1 - \Phi(x) < x^{-1}\phi(x), \quad x > 0.$$

This gives us the final inequality,

$$\frac{d\sigma}{dk}(k) \geq -1 \frac{1}{d_1(k, \sigma(k))},$$

which proves Equation 9. Hence we have proved the lemma.

A.3 Proof of Lemma 3

To prove the first of these results we use the following result from [Lee04], there exists $k^* < 0$ and $\beta \in (0, 2)$ such that,

$$-\frac{\sigma(k)^2}{k} < \beta, \quad k < k^*.$$

Using this we get,

$$\sigma(k) > \sqrt{\beta |k|}$$

for $k < k^*$. This helps us get the following expression,

$$d_2(k, \sigma(k)) = -\frac{k}{\sigma(k)} - \frac{\sigma(k)}{2} > \sqrt{\frac{|k|}{\beta}} - \frac{\sqrt{\beta|k|}}{2} = \frac{2-\beta}{2\sqrt{\beta}}\sqrt{|k|}.$$

We also use that,

$$-d_2(k, \sigma(k)) \geq \sqrt{2k}, \quad k \geq 0.$$

This is proven in the paper [FIM+11] as a Lemma, but we do not prove it here to save space. Thus using both of these we can instantly see that as $|k| \to \infty$ we must have that $\phi(d_2)$ decays exponentially, proving the first result.

To prove the second result we use Lemma 1. This gives us,

$$D(Fe^k) - D_{BS}(Fe^k) = \phi(-d_2(k, \sigma(k)))\frac{d\sigma}{dk}(k).$$

Now using the fact that $D_{BS}(Fe^k) = \Phi(-d_2(k, \sigma(k)))$, we get,

$$\lim_{k\to\infty} kD_{BS}(Fe^k) = 0, \quad \lim_{k\to\infty} k(1 - D_{BS}(Fe^k)) = 0.$$

Also using the integrability of S_T we can get,

$$\lim_{k\to\infty} kD(Fe^k) = 0, \quad \lim_{k\to\infty} k(1 - D(Fe^k)) = 0.$$

These results together prove the second inequality, hence the lemma is proved.